during the left-ankle deep-tendon test and was normal on the right side. The plantar reflex on his left side was positive. Temperature and pinprick responses were decreased below T12; there was hypalgesia below L1 on the left side. Magnetic resonance imaging (MRI) showed a herniated pseudomeningocele and a syringomyelia at the T11/12 level (Figure 1). To show neural structures with increased sensitivity, we used constructive interference in steady-state (CISS) imaging.[3,4] CISS image minimizes the pulsatile cerebrospinal fluid (CSF) by acquiring the sequence with flow compensation applied over each transgressive–regressive cycle (T–R cycle), resulting in a higher intrinsic resolution between neural structures, CSF and lesions surrounded by CSF. In this case, CISS images well demonstrated the attachment of the spinal cord to the wall of a herniated pseudomeningocele; there was a root fiber exiting from the syringomyelia into the herniated pseudomeningocele (Figure 2). On the basis of these preoperative findings, we decided to perform a surgery.

Laminectomy from T11 to T12 revealed a herniated pseudomeningocele adjacent to the T11/12 facet joint. After opening the dura and arachnoid, we noted that the spinal cord was tightly attached to a pale, thick arachnoid tissue inside the herniated pseudomeningocele. The spinal cord was dissected and pulled back into the intradural space (Figure 3). We opened the pseudomeningocele by longitudinal incision. This revealed redundant nerve roots within granulomatous tissue, suggesting nerve root avulsion as the primary lesion. We addressed the swollen spinal cord by 3-mm dorsal root entry zone (DREZ)tomy; this facilitated cerebrospinal fluid (CSF) drainage from the syringomyelia and resulted in the collapse of the syrinx. The involved nerve roots exited from the syringomyelia (Figure 3). A fascia graft was sutured to the dural defect and the area was covered with

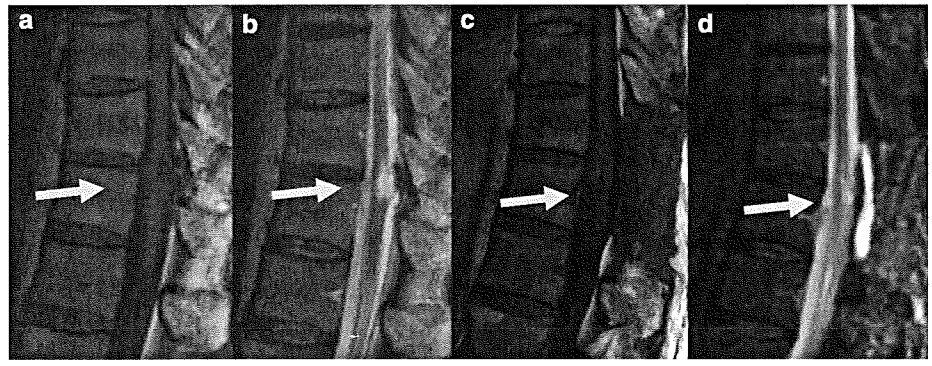

Figure 1 Preoperative magnetic resonance (MR) images ((**a**) Sagittal T1 weighted, (**b**) Sagittal T2 weighted) showed syringomyelia at the T11/12 level. Postoperative MR images ((**c**) Sagittal T1 weighted, (**d**) Sagittal T2 weighted) showed disappearance of the syringomyelia.

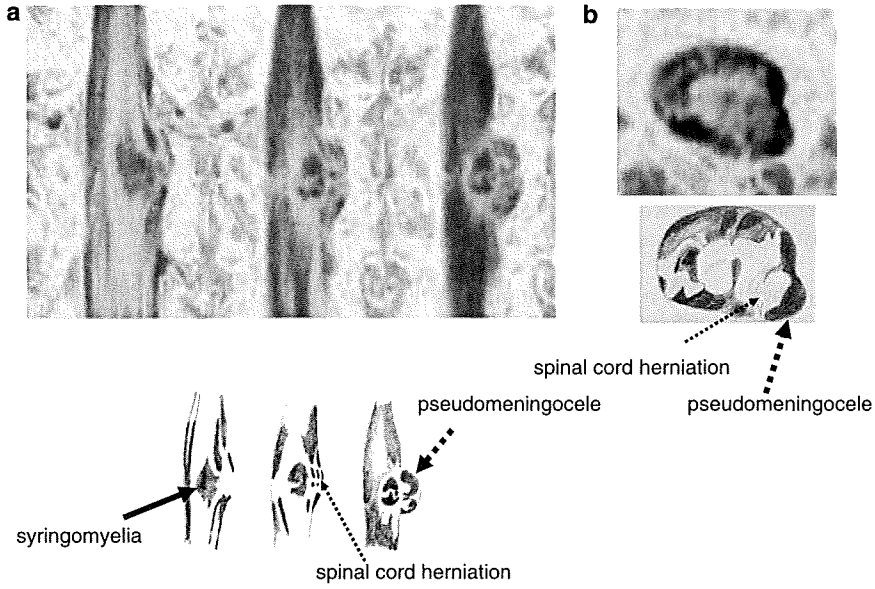

Figure 2 (**a**) Coronal construction interference in steady-state (CISS) images showing syringomyelia, pseudomeningocele and herniation of the spinal cord into the pseudomeningocele. (**b**) Axial CISS images show spinal cord herniation and pseudomeningocele.

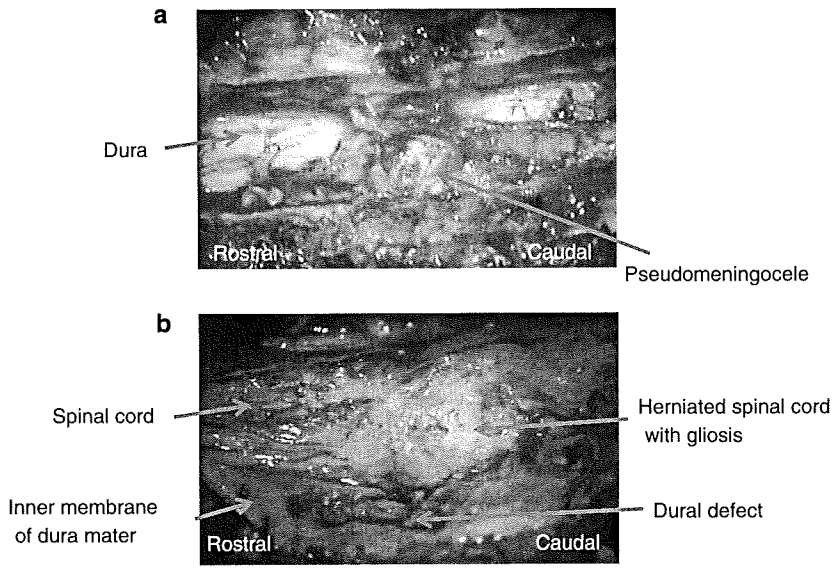

Figure 3 Intraoperative photographs. (**a**) Before opening the dura, a herniated pseudomeningocele was observed adjacent to the T11/12 facet joints. (**b**) After opening the dura and the arachnoid, the herniated spinal cord was dissected and pulled back into the intradural space. Note the dural defect.

a patch sprayed with fibrin glue. Pathological examination of the removed arachnoid tissue disclosed hyalinization.

Postoperative MRI confirmed the disappearance of the cord deviation and intramedullary cyst (Figure 1). Although motor function was remarkably improved, he reported intermittent radiating pain for 6 weeks after surgery; at 10 weeks, it had decreased significantly. At the final observation 1 year after surgery, he had slight numbness in his left thigh without motor dysfunction.

Discussion

Spinal cord herniation is relatively rare; to our knowledge, only 110 cases have been reported to date. Traumatic spinal-cord herniation is extremely rare; our search of the literature disclosed only 13 cases reported earlier.[1,2,5] Although the etiology of spinal cord herniation remains to be established, in most patients with the idiopathic variation the affected levels range between T4 and T7. In patients with traumatic spinal-cord herniation, there was an association with the site of injury.[5] Although most earlier reported patients with traumatic spinal-cord herniation manifested deficits in the ventral or ventrolateral dura mater with tethering of the spinal cord to the dorsal aspect of adjacent vertebrae, dorsolateral spinal-cord herniation was identified in only two, including our patient.

Among the 13 patients reported earlier with traumatic spinal cord herniation, only three were associated with nerve root injury; in all, there was an association with brachial plexus injury. Ours is the first case, in which nerve root injury was associated with a site other than the brachial plexus.

CISS imaging was highly useful for the demonstration of spinal cord herniation, syringomyelia and pseudomeningocele. The sensitivity of CISS sequence is increased in neural tissues because the T_2 values between the CSF and other structures are attenuated, resulting in a higher resolution of CISS images of neural structures. According to the preoperative CISS information, we performed surgical treatment, resulting in clinical improvement.

References

1 DaSilva VR, Al-Gahtany M, Midha R, Sarma D, Cooper P. Upper thoracic spinal cord herniation after traumatic nerve root avulsion. *J Neurosurg* 2003; 99: 306–309.
2 Francis D, Batchelor P, Gates P. Posttraumatic spinal cord herniation. *J Clin Neurosci* 2006; 13: 582–586.
3 Ikushima I, Korogi Y, Hirai T, Yamashita Y. High-resolution constructive interference in a steady state imaging of cervicothoracic adhesive arachnoiditis. *Neuroradiol Comp Assist Tomograph* 2007; 31: 143–147.
4 Ramli N, Cooper A, Jaspan T. High resolution CISS imaging of the spine. *Br J Radiol* 2001; 74: 862–873.
5 Yokota H, Yokoyama K, Noguchi H, Uchiyama Y. Spinal cord herniation into associated pseudomeningocele after brachial plexus avulsion injury: case report. *Neurosurgery* 2007; 60: E205.

内科学症例図説

総編集

杉本恒明

小俣政男

編集

阿部圭志
池田康夫
石井當男
梅村　敏
北村　諭
木村　哲
小池隆夫
白土城照
寺野　彰
名和田新
早川哲夫
福井次矢
松澤佑次
柳澤信夫

朝倉書店

1. 感染症
2. 循環器系の疾患
3. 呼吸器系の疾患
4. 消化器系の疾患
5. 肝の疾患
6. 胆・膵の疾患
7. 膠原病
8. 腎・尿路系の疾患
9. 内分泌系の疾患
10. 代謝の異常
11. 血液疾患
13. 眼底
14. 救急医療

12. 神経疾患

編集 柳澤信夫

12-34 脊髄空洞症

症例　13歳　男性

[臨床所見]

生下時，満期産で吸引分娩であった．2カ月前に左手で氷をもっても，お湯に手を入れても温度を感じないことに気づいた．その後，左上肢のしびれおよび痛みを自覚した．MRI検査にて脊髄空洞症（syringomyelia）と診断され，治療のため当科紹介となった．入院時，神経学的には両上肢のDTRの低下，左C_4-T_2のhypalgesiaをみとめ（**図1**），胸椎で右凸の側彎症をみとめた．

[画像診断]

MRIでは小脳扁桃の下垂とC_{2-}-T_9にsyrinxをみとめた（写真1，2）．syrinxはT_3-T_4にて最大であり，左に偏在していた（写真3）．以上から，Chiari奇形に合併したsyringomyeliaと診断し，症状の進行が速く，空洞のサイズも大きいことから空洞-くも膜下腔交通術（syringo-subarachnoid shunt：S-S shunt）を施行した．

[手術]

手術は腹臥位にて行われた．T_3-T_4に長さ4cmの皮切を行い，T_3-T_4の左側の椎弓に2×1.6cmの椎弓切除（laminectomy）を行った．硬膜を開くと，腫大した脊髄がみとめられ，後根侵入部（dorsal root entry zone：DREZ）が薄く菲薄化していた．菲薄化したDREZに2mmの切開を加えると，空洞内液が噴出し脊髄が縮小した（写真4）．直径1.4mm，長さ40mmのシリコンチューブ（Sapporoシャント）を挿入し，固定した（写真5）．硬膜を縫合閉鎖し，筋肉，皮下，皮膚を縫合し，手術を終えた．

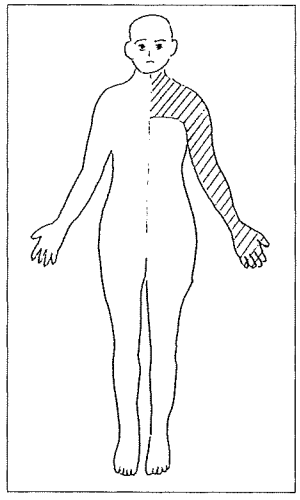

図1
温痛覚障害の部位を示す．

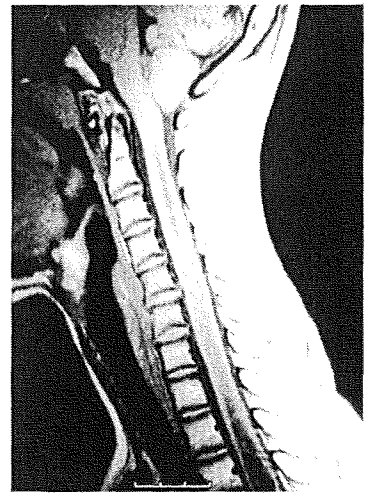

写真1　**頸髄のMRI**
小脳扁桃の下垂，C_2から下の髄内に空洞をみとめる．

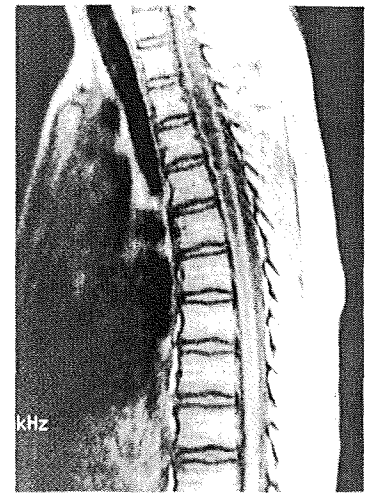

写真2　**脳髄のMRI**
T_9より上の脊髄に空洞をみとめる．

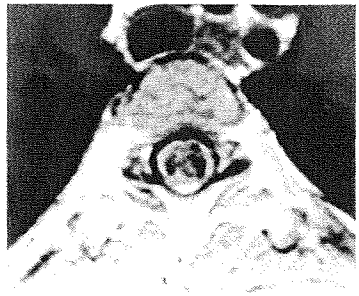

写真3　**T_3-T_4レベルの脊髄**
空洞のサイズは大きいが，左後方に偏在している．

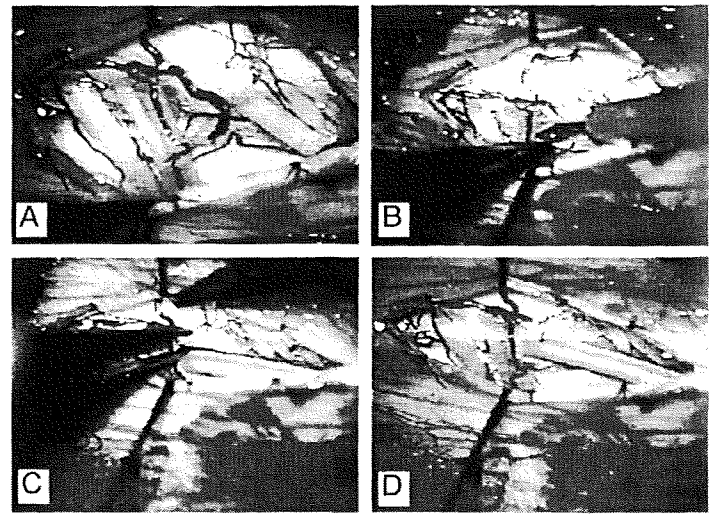

写真4　**硬膜を開いたところ**
A：後根侵入部の脊髄が菲薄化している．B：脊髄に切開を加える．C：S-S shunt tubeを挿入する．D：tubeを固定する．

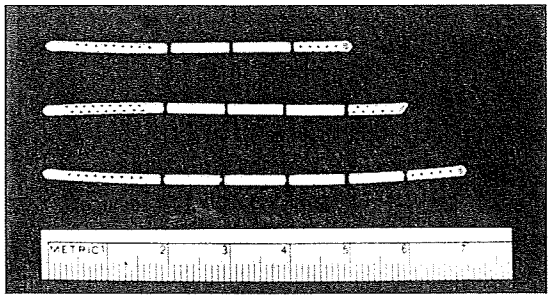

写真5　シリコン製のshunt tube

写真6　術後8日目のMRI矢状断
空洞は著明に縮小している．

［術後経過］

術後，左上肢の痛み，しびれは消失し，左上肢および胸部の温痛覚障害の範囲，程度とも著明に改善した．術8日後のMRIにてsyrinxは著明に縮小しており（写真6），術後10日目に自宅退院となった．

［治療］

脊髄空洞症の手術は大孔部減圧術（foramen magnum decompression：FMD）と空洞くも膜下腔交通術の二つに大別される．前者の治療法が比較的多く施行されているものの，空洞が大きく，症状の進行が急激で，痛みの強い症例では，後者のほうが短時間で空洞の縮小が得られることから有用である．

■飛騨一利

［文献］

Hida K, Iwasaki Y, Koyanagi I, et al: Surgical indication and results of foramen magnum decompresion versus syringo-subarachnoid shunting for syringomyelia associated with Chiari I malformation. *Neurosurgery*, **37**: 673-679, 1995.

岩崎喜信，阿部　弘：Syringomyeliaの手術．脳神経外科，**24**(8)：709-716，1996.